Preparation of silk resins by hot pressing Bombyx mori and Eri silk powders

Preparation of Silk Resins by Hot Pressing *Bombyx mori* Silk and Eri Silk Powders

H.A. Tuan[a*], S. Hirai[b*], Y. Tamada[c] and S. Akioka[d]

[a] *Graduate Student, Muroran Institute of Technology, Japan*

[b] *Research Center for Environmentally Friendly Materials Engineering, Muroran Institute of Technology, 050-8585, 27-1 Mizumoto-cho Muroran-shi Hokkaido, Japan*

[c]*Faculty of Textile Science and Technology, Shinshu University, 386-8567, 3-15-1 Tokida, Ueda City, Nagano, Japan*

[d] *Graduate Student, Muroran Institute of Technology, Japan*

**Corresponding author:*

Email: hoanganhtuan07@gmail.com

hirai@mmm.muroran-it.ac.jp

Abbreviations[1]

[1] SEM Scanning electron microscopy
XRD X-ray diffraction
FT-IR Fourier-transform infrared

Abstract

In this study, silk resins were investigated as alternatives to tortoise shell for eyeglass frames and ornaments. Silk resins were prepared by crushing the raw waste of *Bombyx mori* and Eri silk threads (rather than by scouring and dissolving them) and hot pressing the silk powder in a stainless steel die. The hot pressing was performed at a pressure of 31.2 MPa until the temperature reached a predetermined temperature of 150 °C–180 °C. Because *B. mori* silk powder comprises finer particles than Eri silk powder, the obtained *B. mori* silk resin was denser than the Eri silk resin over a range of resinification temperatures. The micro-Vickers hardness, three-point bending strength, and elastic modulus of the *B. mori* resin reached Hv 60, 112 MPa, and 9.1 GPa, respectively, after 7 days of drying, whereas those in the Eri silk resin were lower (Hv 55, 98 MPa, and 8.5 GPa, respectively). These excellent mechanical properties of *B. mori* silk resin was attributed to its higher apparent density compared with that of Eri silk resin. According to the Fourier-transform infrared spectra, the β-sheet structure content in the *B. mori* silk increased while the random coil structure decreased after the resinification and drying; in contrast, the secondary structure in the Eri silk resin was changed from a random coil to β-strand structure after the resinification process, which was converted to a β-sheet structure after the drying process. However, the β-sheet structure content was similar to the Eri silk and the *B. mori* silk following the resinification and the drying, implying that the differences in the mechanical properties are due to the differing densities of the resins. These findings regarding the fabrication of silk resins are likely to contribute to the future development of useful materials with favorable mechanical properties.

Keywords: Eri silk thread, *Bombyx mori* silk thread, milling powder, hot pressing, resinification, mechanical properties

1. Introduction

The global output of raw silk is increasing due to the demand from high-income countries. Although China supplies the largest quantity of raw silk, Vietnam is the world's sixth largest producer of raw silk after India, Uzbekistan, Thailand, and Brazil [1]. Vietnamese silk products are largely obtained from either *Bombyx mori* silkworms or Eri silkworms. *B. mori* silkworms generally feed on mulberry leaves, whereas Eri silkworms mostly consume cassava leaves [2]. It is known that cassava is easier to cultivate and is useful for other agricultural purposes (e.g., Cassava roots are used as a food product and for ethanol production). Cassava has six cultivation seasons per year, which dramatically increases its annual productivity of raw cocoons compared with mulberry, which has only has one to two cultivation seasons per year. Because Eri silkworms have superior disease resistance and sericulture does not require special technology, it is feasible to produce large amounts of cocoons from small-scale sericulture, which is largely performed by those in Anh Son district, Nghe An province, Vietnam. However, the large number of tubular holes that exist along the thread length and the short fibers of Eri thread makes mechanical spinning impossible [3].

Silk resin has recently been investigated as an alternative to tortoise shell as a material for eyeglass frames and ornaments. Silk resins can be prepared by hot pressing either silk fibroin sheets [4] or silk powder [5]. Fibroin sheets are formed by dissolving silk thread in a hot aqueous calcium chloride solution containing ethanol, casting the desalinated fibroin solution with glycerol, drying, and washing in water to remove the glycerol; then, 30–100 sheets are stacked while immersed in the fibroin solution and hot pressed under a pressure of 19.6–24.6 MPa at 90 °C. After drying at 90 °C,

the maximum bending strength of the laminated silk fibroin sheet is comparable with that of tortoise shell. When preparing silk resin from silk powder, the powder is mixed with water and hot pressed between stainless steel plates with a pressure of 30–80 MPa at a predetermined temperature of 100 °C–190 °C. Silk resin that was prepared by hot pressing silk powder containing 27% water under a pressure of 44 MPa at a temperature of 160 °C for a retention time of 1 h was shown to possess the same hardness as tortoise shell. However, its bending strength was around 70 MPa, which was far short of that of tortoise shell (225–333 MPa).

Our research group introduced a sintering method based on the direct application of a large pulsed electric current to a graphite die [6]. Silk powders loaded onto the graphite die were found to be heated uniformly by internally generated heat due to Joule heating, which occurs when a strong current passes through the contact points between compacted particles. Moreover, the Joule heat can be generated at many points dispersed throughout the sample by repeatedly switching the voltage and current on and off. By this approach, uniform parts can be compacted more quickly than through the use of conventional hot pressing. In the previous study, silk powder was obtained by dissolving scoured silk thread in an aqueous solution of a neutral salt, desalination, and freeze drying; the obtained silk powder was then treated by the proposed pulsed electric current sintering method at a pressure of 20–30 MPa at a temperature of 150 °C–170 °C. The results showed that the obtained silk resin possessed a thermal conductivity of 0.44 W/(m·°C) (which is extremely high for a resin [7]), a glass transition temperature of 180 °C, a bending strength of 100 MPa, and a bending elastic modulus of 4.5 GPa.

In this study, we aimed to fabricate silk resins using an easier method than the pulsed electric current sintering method. The raw silk powder was prepared from silk threads, which are normally wasted by crushing rather than by scouring and dissolving, as is traditionally done for this purpose. Two types of silk threads are investigated: silk from the Vietnamese domesticated *B. mori* silkworm and silk from the *Samia cynthia ricini* (or Eri) silkworm. Resins were prepared by hot pressing followed by drying. The mechanical properties of the resins were characterized. Specifically, the effects of drying after hot pressing on the three-point bending strength, micro-Vickers hardness, elastic modulus, water content, and apparent specific density of each resin were investigated. Moreover, X-ray diffraction (XRD), Fourier-transform infrared (FT-IR) spectroscopy, and high-performance liquid chromatography were used to explain the effects of the resinification and drying processes in terms of the structural characteristics.

2. Materials and methods

Figure 1 shows a flowchart describing the process used to prepare the silk resins. Eri silk thread and *B. mori* silk threads were milled and sieved to obtain silk powders, which were then hot pressed and dried to obtain the silk resins. This process is described in detail as follows.

2.1. Silk Powders

Raw Eri silk thread and *B. mori* silk thread were collected before degumming by the Vietnam Sericulture Research Center and used as the raw material in this study. The Eri silk thread was

sourced from the ethnic minority in Vietnam. To prepare the silk powders, the Eri and *B. mori* silk threads were crushed using a planetary ball mill (Pulverisette 6, Fritsch, Germany) with a 500-mL alumina pot and φ15 and φ20 mm alumina balls with a total weight of 3.2 kg. The crushed silk powders had fiber lengths in the range of 1–3 mm. Then, 2 g of the 3.2-kg crushed power sample was milled at a rotational speed of 300 rpm for 15 cycles, each including 1 min of milling time, 5 min of waiting time, and 1 min of reverse rotation. The milled silk powders were then sieved in a vibratory sieve shaker (AS200, Retsch, Germany) at 60 beats per minute for 60 min to obtain a silk powder with particles smaller than 50 μm. The mean particle sizes of the silk powders were confirmed by a laser diffraction particle size analyzer (SALD2300, SHIMADZU, Japan).

2.2. Resinification

Silk powder was loaded into a stainless steel die with the diameter of 20 mm for compaction by a hot press (H300-05, AS One, Japan) until the temperature reached a predetermined temperature (called the resinification temperature); the assembly was then allowed to cool. Because the mechanical properties were found to be consistent in the pressure range from 20 to 40 MPa, 31.2 MPa was chosen as the pressure for the resinification process. Several resinification temperatures in the range of 150 °C–180 °C were tested. The samples were dried at 100 °C in a vacuum for different lengths of time from 3 to 7 days.

2.3. Three-Point Bending Test and Micro-Vickers Hardness Test

Small plate-shaped test pieces of 3 mm in width, 12 mm in length, and 2.5 mm in thickness were

cut from the compacted silk resin samples. Three-point bending tests were conducted on a universal tensile testing machine (Autograph AGS-X series, SHIMADZU, Japan) with a support interval of 10 mm and a testing speed of 0.5 mm/min^{-1}. The maximum strength before failure was measured three times, and the average result was considered herein. The bending elastic moduli of the samples were calculated from their stress–strain curves. The hardness of each resin section was measured using a micro-Vickers hardness meter (HMV-G series, SHIMADZU, Japan), and the following equation was used to convert the results from Vickers Hardness (Hv) units to the SI units (MPa): MPa = 9.80 × Hv.

2.4. Structural Analysis

The water contents in the silk powders and resins were measured by Karl Fischer titration (860 KF Thermoprep, Metrohm AG, Herisau, Switzerland). The apparent densities of the samples were measured by the Archimedes method using an analytical balance (AUX120, SHIMADZU Co., Japan). The structure of the resin was characterized in small cut samples of 10 × 10 mm using XRD (Ultimat IV, Rigaku Corp., Japan) and FT-IR spectroscopy (FT-IR-6600, Jasco Corp., Japan). The XRD was conducted using a CuKα ray with tube conditions of 40 kV and 40 mA. The fractured resin sections from the three-point bending tests were observed using scanning electron microscopy (SEM) (JSM-6610LA, JEOL Ltd., Tokyo, Japan).

2.5. Amino Acid Analysis

To characterize the amino acids in the fibroin samples, it was first necessary to hydrolyze the peptide bonds in the silk fibroin powders and resins using a 4-mol/L methanesulfonic acid solution. Then, an automated amino acid analysis was conducted with 0.2 wt% 3-(2-Aminoethyl) indole (Wako Pure Chemical, Japan) as the acid catalyst at 110 °C for 24 h using a high-speed amino acid analyzer (AL-8800, Hitachi, Japan).

3. Results and Discussion

3.1. Resinification and Densification

Figure 2 shows the particle distributions in the silk powder after the sieving process. The columns represent the frequencies of the particle sizes (%), and the lines represent the integration of this distribution (%) in the silk powder. Figure 3 (a) and (b) shows SEM images of the powders after sieving. The most frequent particle size in the distribution was around 60 μm in both silk powders; other peaks were observed at 1 and 0.5 μm in the particle size distributions for the Eri and *B. mori* silk powders, respectively. It has been reported that the tensile strength (elastic modulus) and elongation for *B. mori* silk thread are 4.3–5.2 g/denier (84–121 g/denier) and 10.0%–23.4%, respectively, whereas those for Eri silk thread are 1.9–3.5 g/denier (29–31 g/denier) and 24%–27%, respectively [8]. Thus, it has been hypothesized that further milling of the powder beyond particle sizes in the range of 60–70 μm was prevented by the cushioning effect [9], which notably results in

softening of the material. Figure 3 (c) and (d) shows the fracture surfaces of the 150-^{o}C hot-pressed resin samples after the three-point bending test. The fracture surface of the Eri silk resin reveals the presence of micro-fibers inside the resin, which are expected to directly affect the apparent density and mechanical properties of the resin. However, the *B. mori* resin exhibits a typical brittle fracture surface.

Figure 4 shows the water content and the apparent density of the resins as functions of the resinification temperature during hot pressing. After hot pressing, the water content of the Eri silk resin was reduced dramatically from 12 mass% to about 7.7 mass% whereas that of *B. mori* silk also decreased (though less significantly) from 11.7 mass% to about 9.1 mass%. It has been reported that *B. mori* silk powder undergoes partial dissolution in water at the time of resinification in the presence of high-temperature steam and is homogeneously resinified [6]. Since the silk powders used in this study contained sufficient water content to facilitate this process, the addition of water was not required. Moreover, the water content in the resin was found to be independent of the resinification temperature. However, the apparent density of the *B. mori* silk resin was greater than that of the Eri silk resin over the entire range of resinification temperatures tested.

As described in Figures 1 and 2, *B. mori* silk powder comprises finer particles than Eri silk powder; densification occurs because of the semi-fusion state that is formed in the presence of fine particles. In addition, the apparent density of the *B. mori* silk resin samples increased as the resinification temperature increased whereas that of the Eri silk resin decreased with increasing resinification temperature. In general, since it is easy to densify the sample such that its

resinification temperature increases, a higher density, such as that of the *B. mori* silk resin, is desirable. However, in the Eri silk resin, some of the water required to maintain a semi-molten state evaporated during a hot-pressing process due to the coarse particle size of the Eri silk powder and the remaining micro-fibers; overall, it was concluded that the resin from Eri silk did not exhibit sufficient densification. Moreover, because of the intense evaporation of moisture causing a moisture shortage in the samples treated with higher resinification temperatures, the resin densification was also considered insufficient in these samples.

Figure 5 shows the water contents and apparent densities of the resins as functions of the drying time when the resinification temperature was fixed to 150 °C. In both resins, the water content decreased with longer drying times, falling as low as 0.5 wt% by day 7. Moreover, the water content in the Eri silk resin with low density and insufficient densification decreased more quickly than in the *B. mori* silk resin. This was attributed to the formation of pores in the Eri silk resin that allows water to pass through the structure.

3.2. Mechanical Properties of Resins

Figure 6 shows the relationship between the mechanical properties of the silk resins that were hot pressed at 150 °C as functions of the drying time. The data show that the longer the drying time was, the more the micro-Vickers hardness, three-point bending strength, and elastic modulus of the resin increased. Moreover, the mechanical properties of the Eri silk resin were inferior to those of the *B. mori* silk resin at all drying temperatures. Specifically, the *B. mori* and Eri silk resins exposed to the longest drying time of 7 days had the highest mechanical properties: three-point bending

strengths of 112 and 98 MPa, respectively, elastic moduli of 9.1 and 8.5 GPa, respectively, and micro-Vickers hardness values of Hv 60 and Hv 55, respectively. These mechanical properties represent significant improvements over those attained in previous studies [4–6,10]. These excellent mechanical properties of *B. mori* silk resin were attributed to the higher apparent density of *B. mori* silk resin compared with Eri silk resin. Thus, the mechanical properties of the resins are considered to depend on their densification and resinification transformation.

3.3. Structural Analysis

The XRD spectra obtained from the silk powders and silk resins fabricated at a constant temperature of 150 °C are shown in Figure 7. Both spectra show amorphic phasess [11], [12] and present and demonstrate the formation of crystalline phases [12]. The crystal structure of the Eri silk II was characterized by peaks at 16.4°, 19.3°, and 23.8°, whereas the *B. mori* silk II exhibited peaks at 18.0°, 20.2°, and 24.0° [13]. The differences between these diffraction peaks were attributed to the differences in the unit cell dimensions in these materials [14]. The intensities of the crystal peaks were increased after drying for 7 days in parallel with the increase in the mechanical properties. This is considered to be because the residual water leaving the resins was in the bound water form. During this process, the secondary structure of the resin was pleated from small stacked β-pleated-sheet crystal to bigger stacked β-pleated-sheet crystal [15]. These findings are consistent with previous reports, demonstrating that water impacts the strength of a crystallite structure as it reduces the number of hydrogen bonds, the hydrogen bond lifetime, and the peak rupture force and increases the specific interaction energy [16]. This also explains why the mechanical properties of

resins were increased after the drying process.

Figure 8 shows the FT-IR spectra, which indicate that the changes in the fibroin's secondary structure after the hot pressing and drying. The secondary derivatives that can be used to characterize the secondary structure of Amide I are shown in Figure 9. It has been reported that Eri silk without sericin exhibits absorption bands at 1649 cm^{-1} (amide I), 1559 and 1523 cm^{-1} (amide II), and 1233 cm^{-1} (amide III). On the other hand, *B. mori* silk fibers without sericin showed intense absorption bands at 1643 cm^{-1} (amide I), 1509 cm^{-1} (amide II), and 1127 cm^{-1} (amide III) [17]. In the obtained secondary derivatives, the absorption peaks at 1633 cm^{-1} (amide I), 1515 cm^{-1} (amide II), and 1233 cm^{-1} (amide III) were attributed to the formation of a β-sheet structure in the fibroin of the Eri silk powder. The peaks at 1641 cm^{-1} (amide I) were indicative of a random coil structure, and those at 1515 cm^{-1} (amide II) and 1231 cm^{-1} (amide III) were indicative of a β-sheet structure in the *B. mori* silk powder. In the spectra of the Eri silk resin, the peaks in the amide I and amide III bands shifted to lower wavenumbers simultaneously. In the spectra of *B. mori* silk resin, the peaks of the amide I band shifted to a lower wavenumber, whereas the peaks of the amide II and amide III bands did not change. Thus, it was concluded that the secondary structure of the resins did not change significantly upon removal of the water by drying.

On the basis of the secondary derivatives method used previously [18], the component peaks were identified via the curve fitting process as shown in Figure 9. In a previous study [19], it was reported that the β-sheet structure is characterized by a strong absorption peak at 1633.41 cm^{-1} and a relatively weak peak at 1698.02 cm^{-1} and the random coil structure is characterized by absorption

peaks at 1644.98 and 1651.73 cm^{-1}; moreover, absorption peaks at 1668.12, 1673.91, 1681.62, and 1688.37 cm^{-1} are indicative of a β-turn structure, peaks at 1604.48 and 1611.23 cm^{-1} represent a side chain structure, a peak at 1618 cm^{-1} indicates a β-strand structure, and a peak at 1660.41 cm^{-1} represents an α-helix structure.

Table 1 shows the amide I components determined on the basis of the secondary derivatives in Figure 8. The β-sheet structure in the *B. mori* silk increased while the random coil structure decreased after resinification and drying. This means that the secondary structure of the *B. mori* silk was converted from a random coil structure to a β-sheet structure. Meanwhile, the secondary structure of the Eri silk resin was converted from a random coil structure to a β-strand structure upon resinification process and the β-strand structure transitioned into a β-sheet structure upon drying. It is well known that presence of a β-sheet structure influences the bending properties of the material [16]. As there are no differences between the β-sheet structure contents in Eri and *B. mori* silk resins after the resinification and drying, it is clear that observed differences in their bending properties are to the density differences.

Table 2 shows the amino acid compositions of silk powders and silk resins. The amino acids composition was unchanged upon resinification in both resins. The main amino acids in the *B. mori* silk included glycine and serine, which are hydrophilic amino acids; these were more abundant in the *B. mori* silk than in the Eri silk. Accordingly, the ratio of hydrophobic amino acids to hydrophilic amino acids was higher in the Eri silk resin than in the *B. mori* silk resin. Because the *B. mori* silk powder contains a large proportion of hydrophilic amino acids and has fewer

hydrophobic β-sheet structures, it exhibits strong hydrophilic properties. Thus, it is assumed that the hydrophilic amino acids in the *B. mori* silk contribute to the higher apparent density of the resin.

4. Conclusions

The highest three-point bending strength of 112 MPa and the highest elastic modulus of 9.1 GPa were obtained in the *B. mori* resin that was prepared by hot pressing the raw silk powder at 150 ºC. These values were higher than those in the resins that were prepared by a pulsed electric current sintering method with refined silk. The *B. mori* silk resins exhibited higher apparent densities, bending strengths, and micro-Vickers hardness values compared with the Eri silk resins. On the basis of the FT-IR spectra of *B. mori* silk, the β-sheet structure was formed while the random coil structure was broken down upon resinification and drying. On the other hand, the secondary structure of the Eri silk resin was converted from a random coil structure to a β-strand structure upon resinification and β-strand structure was converted to a β-sheet structure upon drying. However, because there was no difference between the β-sheet structure contents in the Eri and *B. mori* silk resins after resinification and drying, it can be concluded that the observed differences in the bending properties are related to the density of the resin.

5. Acknowledgment

This work was supported by Super High-Function Structure Proteins to Transform the Basic Materials Industry of ImPACT (Impulsing Paradigm Change through Disruptive Technologies

Program), Japan.

6. References

[1] FAO, “FAOSTAT_data_3-8-2018 (Livestock Primary),” 2018.

[2] N.Sakthivel, “Evaluation of Cassava Varieties for Eri Silkworm , Samia Cynthia Ricini,” *Mun. Ent. Zool.*, vol. 11, no. March, pp. 165–168, 2016.

[3] S.Prasong, S.Wilaiwan, and S.Yaowalak, “Cross-section images of Eri (Samia ricini) - silk fibers and their secondary structures after treatment with different organic solvents,” *J. Biol. Sci.*, vol. 11, no. 1, pp. 46–51, 2011.

[4] J.Hosokawa, T.Endo, M.Nishiyama, T.Morita, and M.Funahashi, “Development of Turtleshell-Work-Materials Using Silk Protein - Thermal and Mechanical Properties of Turtleshell and Hotpressed Fibroin,” *Kobunshi Ronbunshu*, vol. 50, no. 12, pp. 929–934, 1993.

[5] J.Hosokawa, T.Endo, R.Kitagawa, and A. M.Nishiyama, “Properties of novel ornamental material boards made from silk fibroin sheet,” *J. Chem. Eng. Japan*, vol. 29, no. 6, pp. 1057–1059, 1996.

[6] A.Kaneko, Y.Tamada, S.Hirai, T.Kuzuya, and A. T.Hashimoto, “Characterization of a Silk-Resinified Compact Fabricated Using a Pulse-Energizing Sintering Device,” pp. 272–278, 2012.

[7] “Japan Patent JP.04-029766.B.”

[8] B.Kundu, R.Rajkhowa, S.Kundu, and X.Wang, “Silk fibroin biomaterials for tissue regenerations,” *Adv. Drug Deliv. Rev.*, vol. 65, no. 4, pp. 457–470, 2013.

[9] M.Kazemimostaghim, R.Rajkhowa, K.Patil, T.Tsuzuki, and X.Wang, “Structure and characteristics of milled silk particles,” *Powder Technol.*, vol. 254, pp. 488–493, 2014.

[10] W.Yu, T.Kuzuya, S.Hirai, and Y.Tamada, “Fabrication of Silk Resin Sheets Using a Hot-Rolling Equipment Division of Engineering for Composite Functions,” *Sen’i Gakkaishi*, vol. 60, pp. 259–264, 2012.

[11] G.M.Nogueira *et al.*, “Preparation and characterization of ethanol-treated silk fibroin dense membranes for biomaterials application using waste silk fibers as raw material,” *Bioresour. Technol.*, vol. 101, no. 21, pp. 8446–8451, 2010.

[12] M. Kazemimostaghim, R. Rajkhowa, and X. Wang, “Comparison of milling and solution approach for production of silk particles,” *Powder Technol.*, vol. 262, pp. 156–161, 2014.

[13] S.Dutta, B.Talukdar, R.Bharali, R.Rajkhowa, and D.Devi, “Fabrication and Characterization of Biomaterial Film from Gland Silk,” *Biopolymers*, vol. 99, no. 5, pp. 326–333, 2012.

[14] J.O.Warwicker, “Comparative studies of fibroins,” *J. Mol. Biol.*, vol. 2, no. 6, pp. 350–362, 1960.

[15] X.Hu, D.Kaplan, and P.Cebe, “Dynamic Protein and Water Relationships during b-Sheet Formation,” *Macromolecules*, vol. 41, pp. 3939–3948, 2008.

[16] Y.Cheng, L.-D.Koh, D.Li, B.Ji, M.-Y.Han, and Y.-W.Zhang, “On the strength of β-sheet crystallites of Bombyx mori silk fibroin,” *J. R. Soc. Interface*, vol. 11, no. 96, 2014.

[17] S.Prasong, S.Yaowalak, and S.Wilaiwan, “Characteristics of silk fiber with and without sericin component a comparision between Bombyx mori.pdf,” *Pakistan J. Biol. Sci.*, vol. 12,

no. 11, pp. 872–876, 2009.

[18] H.Susi and D.M.Byler, “Protein structure by Fourier transform infrared spectroscopy: Second derivative spectra,” *Biochem. Biophys. Res. Commun.*, vol. 115, no. 1, pp. 391–397, 1983.

[19] X.Hu, D.Kaplan, and P.Cebe, “Determining beta-sheet crystallinity in fibrous proteins by thermal analysis and infrared spectroscopy,” *Macromolecules*, vol. 39, no. 18, pp. 6161–6170, 2006.

Biography of Author

	Hoang Anh Tuan was born in Hanoi (Vietnam) in 1986. He graduated in Material Engineering from Hanoi University of Science and Technology (HUST) in 2010. In 2010-2014, Hoang worked in RITM in Hanoi (Vietnam) and studied titanium base alloys as biomaterials, HSLA steel for aviation technique which belong to Vietnamese Government projects. In 2012-2014, he was attended to Master course of HUST, where as part of his thesis he conducted research in the titanium base alloys as biomaterials under the supervision of Associate Professor Pham Mai Khanh. In 2016, he played a role in a Ph.D student to carry out the research into "Development of functional Bio-resins by using the waste clothes resources" in Professor Hirai Shinji's laboratory, Muroran Institute of Technology-Japan.
	Shinji Hirai obtained his Ph.D. in Engineering from Waseda University (Japan) in 1988. In 1990, he joined the Department of Materials Science and Engineering, Muroran Institute of Technology as an Associate Professor. In 1992–1993, he trained under Professor Emeritus L. Brewer at the UC Berkeley. In 2003, he acquired the position of Full Professor and his research interests expanded to include effective utilization of rare earth sulfides and high-performance biomass plastics created using animal fiber waste. Since 2012, he is concurrently serving as the Director, Research Center for Environmentally Friendly Materials Engineering. Recently, as part of the ImPACT national project, he is involved in the study of resinification of artificial spider silk.
	Yasushi Tamada received his B.S. and M.S. from the Department of Polymer Chemistry, Faculty of Engineering, Kyoto University, Japan, in 1983. He completed his Doctor degree in the same department, Kyoto University, in 1989. In his Doctor thesis, he has studied the interaction between polymer surfaces and cells to develop polymeric biomaterials for medical device applications. His research carrier has started in the polymer industry, Japan Synthetic Rubber (JSR) Co. Ltd. in 1987, where he participated several different projects concerning the biomedical devices. He joined National Institute of Sericultural and Entomological Sciences in Tsukuba in 1997, and then started the new research field related to silk materials. He was promoted to the head of silk materials research unit at National Institute of Agrobiological Sciences in 2000, and then moved to the Faculty of Textile Science and Technology, Shinshu University, Ueda, Japan, as a full professor in

	2013. He was awarded the prize of the Japanese Society of Silk Science in 2012.
	Shota Akioka was born in Sapporo, Hokkaido (Japan) in 1991. He graduated from Muroran Institute of Technology in 2014 and master course of there in 2016 under supervising of Professor Hirai Shinji. He carried out the research for fabrication of material using protein “fibroin” including silk in 2013-2016. In 2016-2017, he studied about Bio-materials as structural material in a company involved participating in the national project. From 2018 until now, he continues researching the materials using animal’s protein as the doctor’s student of Muroran Institute of Technology.

Highlights

1. The highest mechanical properties of *B. mori* resin were 112 MPa and 9.1 GPa for three-points bending and Young's Modulus, respectively, prepared by hot pressing at 150 ºC.
2. This kind of resins were higher than those resins made by a pulsed electric current sintering method with refined silk.
3. The secondary structure of silk fibroin was converted from random coil to β-sheet after the resinification process.
4. The mechanical properties of the resins are considered to depend on their densification and resinification transformation.

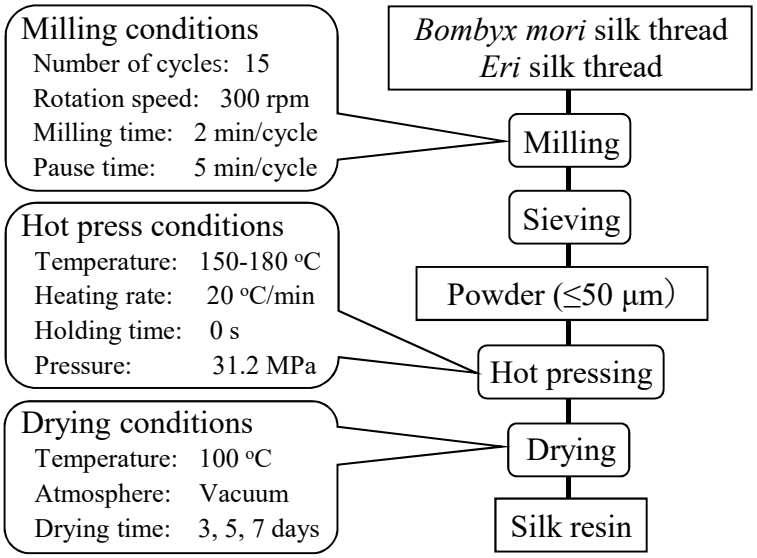

Figure 1 Process of preparing silk resins.

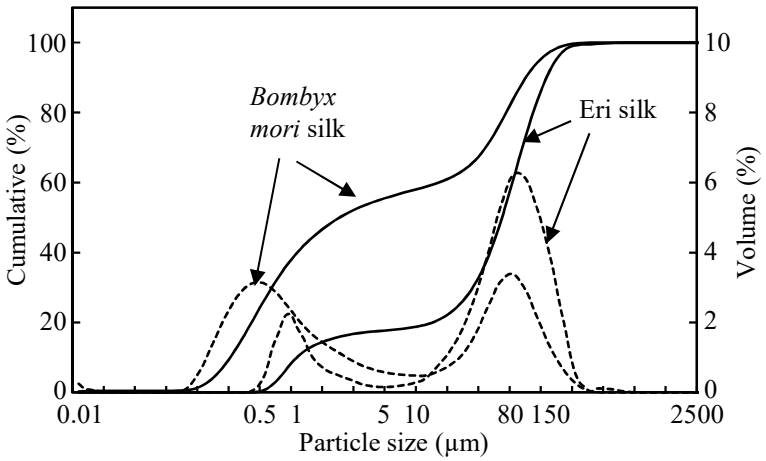

Figure 2 Particle-size distributions in the silk powders after sieving. The solid lines represent the cumulative volume distributions and the dotted lines represent the particle volume distributions.

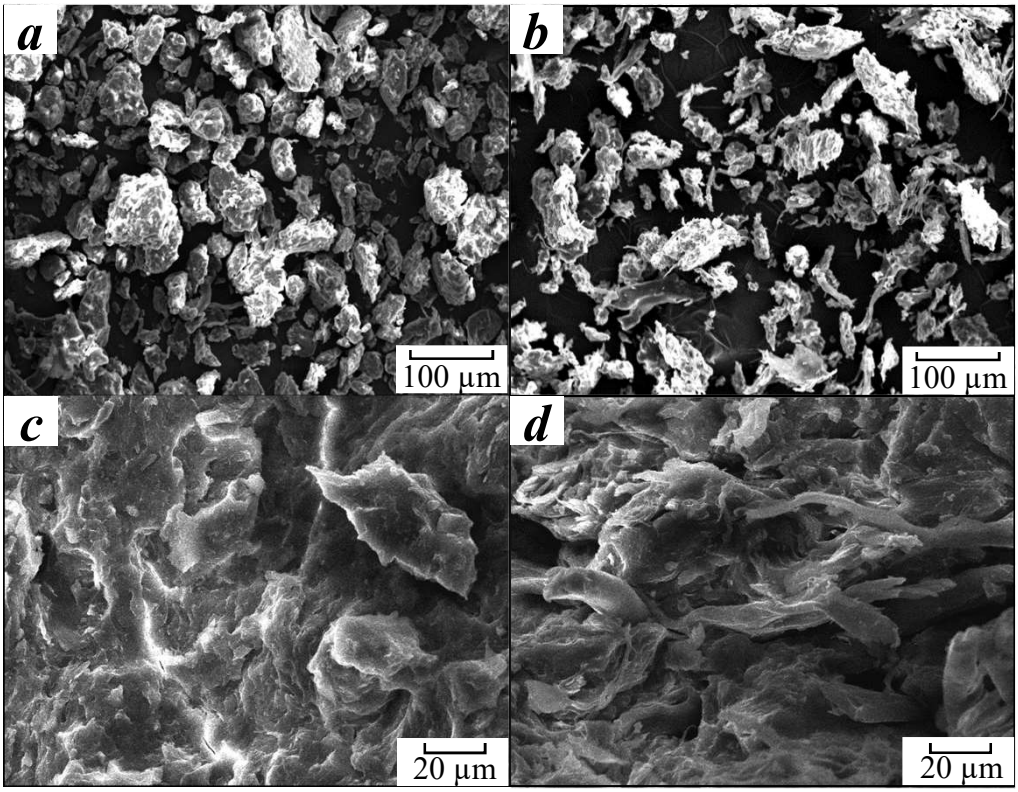

Figure 3 SEM images of (a) the *Bombyx mori* silk powder and (*b*) the Eri silk powder after sieving and the fracture surfaces of (*c)* the *B. mori* silk resin and (d) the Eri silk resin.

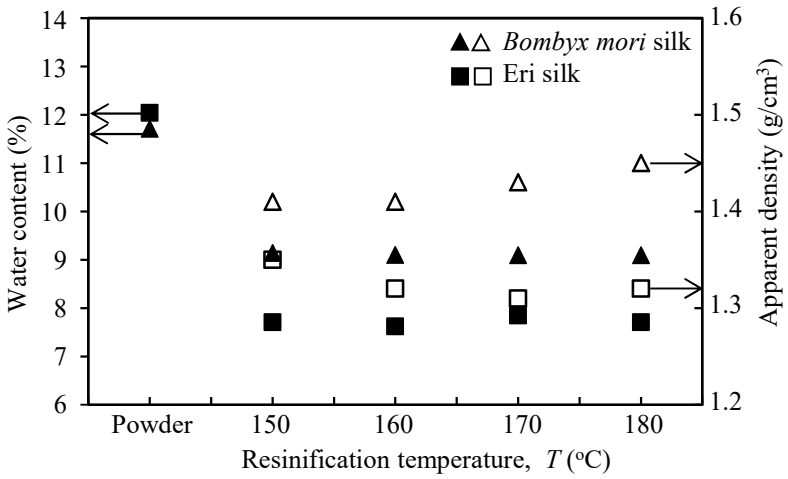

Figure 4 Water content and apparent density of the two resins as functions of the resinification temperature during hot pressing.

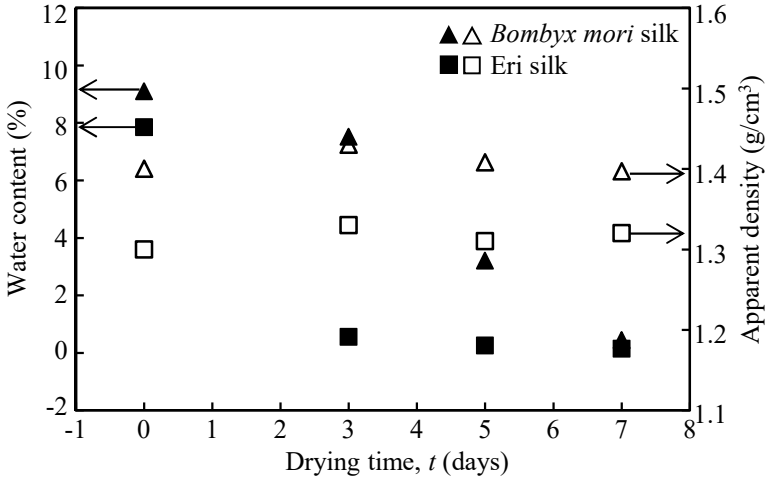

Figure 5 Drying time dependences on the water content and apparent density of resins when a resinification temperature is fixed to 150 ℃ under a pressure of 20 MPa.

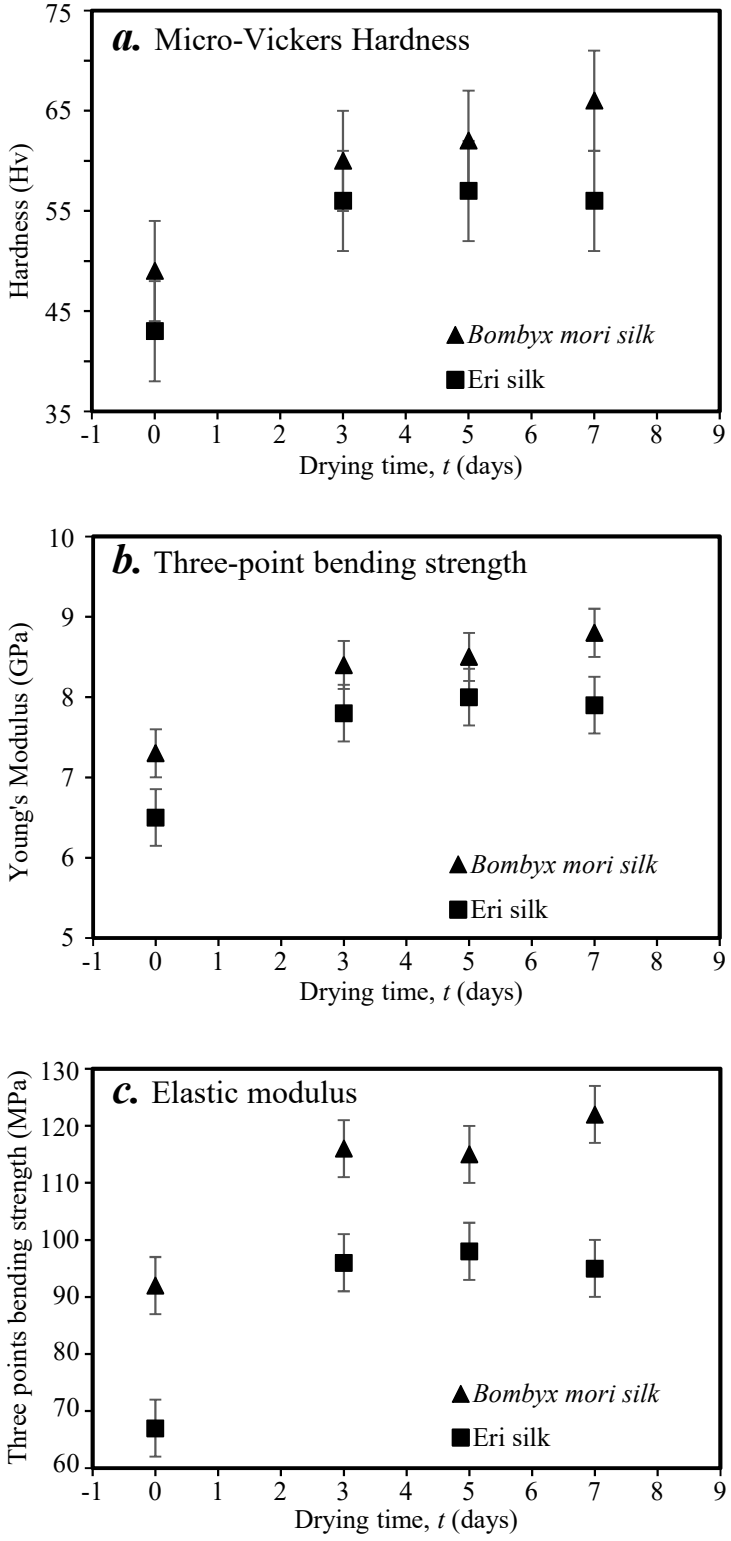

Figure 6 Relationships between the mechanical properties and the drying time for the silk resins that were hot-pressed at a 150 ℃.

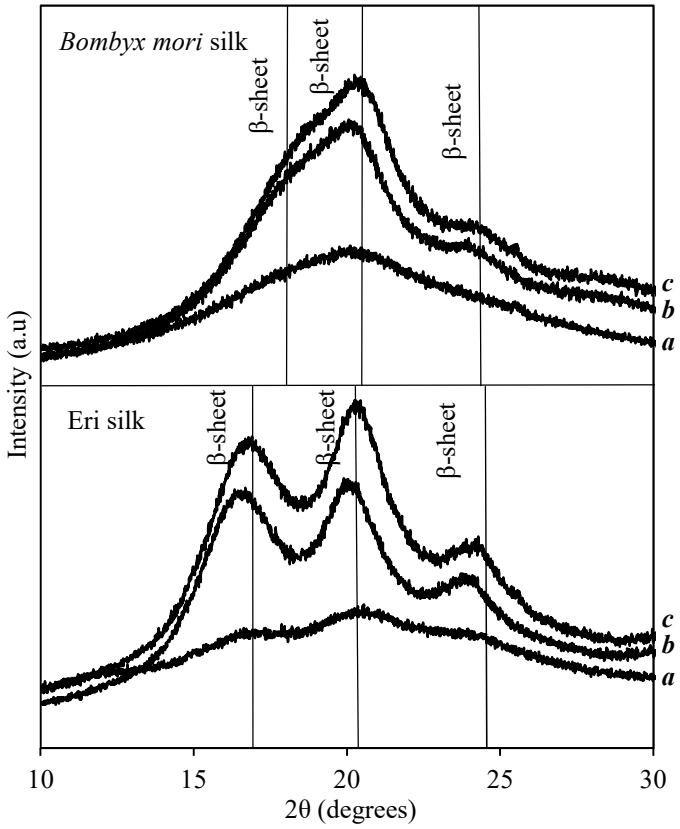

Figure 7 XRD spectra of (a) the silk powders, (b) the resins, and (c) the resin after drying for 7 days when the resinification temperature was fixed at 150 ℃ with a pressure of 20 Mpa.

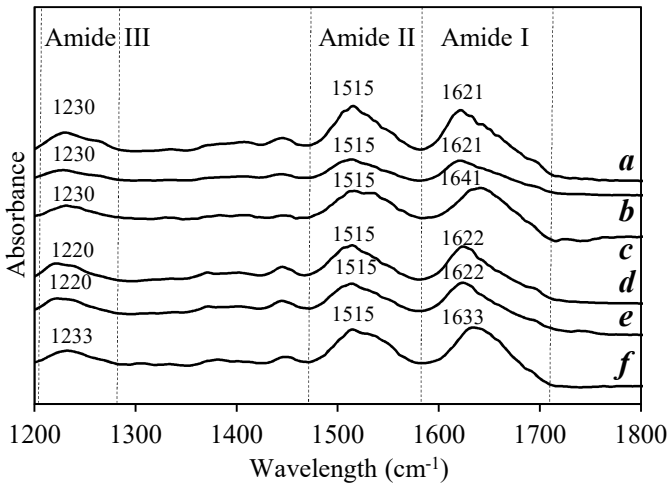

Figure 8 FT-IR spectra of the silk powders and resins when the resinification temperature was fixed to 150 ℃ with a pressure of 20 MPa: (*a*) *Bombyx mori* silk powder, (*b*) *Bombyx mori* silk resin, (*c) Bombyx mori* silk resin after drying for 7 days, (*d*) *Eri* silk powder, (*e*) *Eri* silk resin, and (*f*) *Eri* silk resin after drying for 7 days.

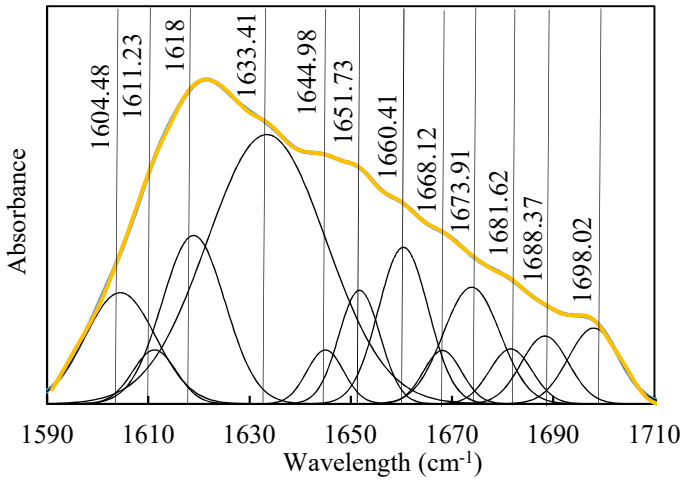

Figure 9 Curve fitting to the FT-IR spectra by using the secondary derivatives to determine the secondary of amide I.

Table Legends

Table 1 The secondary structure content (%) of Amide I of Bombyx mori silk and Eri silk

Assignment		α helix	β strand	β sheet	RC	β turn	SC
Bombyx mori silk	Powder	21.7	4.5	25.4	22.0	18.5	7.9
	Resin	5.1	4.3	36.6	12.4	18.9	22.7
	Resin dried	9.2	12.4	42.1	7.8	16.7	11.8
Eri silk	Powder	12.9	4.6	34.8	19.5	21.1	7.1
	Resin	8.8	11.6	34.2	9.2	15.9	20.3
	Resin dried	6.3	7.4	44.9	16.9	17.1	7.5

Table 2 Amino acids composition of Bombyx mori silk and Eri silk powder and resins

Amino Acids		*Bombyx mori* silk		Eri silk	
		Powder	Resin	Powder	Resin
Hydrophilic	Pro	0.56	0.56	0.41	0.42
	Gly	38.64	38.50	31.24	31.44
	Ser	14.56	14.48	6.97	6.98
	Glu	1.91	1.92	0.92	0.92
	Asp	4.78	4.81	4.12	4.12
	Cys	0.20	0.17	0.09	0.08
	Thr	2.55	2.55	0.51	0.52
	Lys	0.84	0.79	0.26	0.27
	His	0.49	0.47	1.26	1.26
	Arg	1.07	1.07	1.98	1.97
Hydrophobic	Ala	25.21	25.30	45.17	44.75
	Met	0.07	0.08	0.01	0.01

Val	2.60	2.62	0.61	0.60
Phe	0.68	0.67	0.23	0.23
Ile	0.69	0.69	0.38	0.38
Leu	0.68	0.68	0.37	0.37
Tyr	4.45	4.59	5.42	5.63
Hydrophobic/hy-drophilic ratio	2.23	2.23	3.64	3.59
Basic amino acid (mol%)	2.4	2.33	3.5	3.5
Acidic amino acid (mol%)	6.69	6.73	5.04	5.04
Basic/acidic ratio	0.36	0.35	0.69	0.69